Science of the Total Environment 897 (2023) 165364

Contents lists available at ScienceDirect

Science of the Total Environment

journal homepage: www.elsevier.com/locate/scitotenv

Integrated LiDAR-supported valuation of biomass and litter in forest ecosystems. A showcase in Spain

Adrián Pascual [a,*], Sergio Godinho [b], Juan Guerra-Hernández [c]

[a] *Department of Geographical Sciences, University of Maryland, College Park, MD 20742, United States of America*
[b] *Department EaRSLab—Earth Remote Sensing Laboratory, University of Évora, Évora, Portugal, iInstitute of Earth Sciences (ICT), Universidade de Évora, Évora, Portugal*
[c] *Forest Research Centre, School of Agriculture, University of Lisbon, Tapada da Ajuda, 1349-017 Lisbon, Portugal*

HIGHLIGHTS

- The evaluation of total biomass in forests is important for mitigation.
- High-resolution biomass mapping must scope multiple biomass components.
- We used airborne laser data and field measurements over 2 million ha in Spain.
- Good estimation of belowground biomass using aboveground for modelling
- Relations between litter, below-and aboveground biomass depend on forest type.

GRAPHICAL ABSTRACT

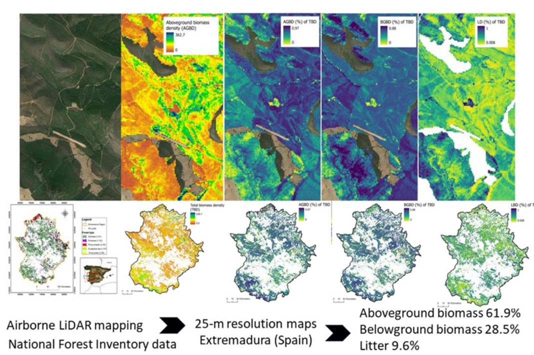

ARTICLE INFO

Editor: Manuel Esteban Lucas-Borja

Keywords:
Airborne laser scanning
Mitigation
Forest modelling
Carbon

ABSTRACT

Belowground components (biomass and soils) can stock as much carbon as the aboveground component of forest ecosystems. In this study, we present a fully-integrated assessment of the biomass budget and the three pools evaluated: aboveground (AGBD) and belowground biomass in root systems (BGBD) and litter (LD). We turned National Forest Inventory data, airborne Light Detection and Ranging (LiDAR) data actionable to map three biomass compartments at 25-m resolution over more than 2.7 million ha of Mediterranean forests in the South-West of Spain. We assessed distributions and balanced among the three modelled components for the entire region of Extremadura and specifically for five representative forest types. Our results showed belowground biomass and litter represent an important 61 % of the AGBD stock. Among forest types, AGBD stocks were the dominant pool in pine-dominated areas while its lowers contribution was found over sparse oak forests. The three biomass pools estimated at the same resolution were used to produce ratio-based indicators to highlight areas where the contribution of belowground biomass and litter can exceed AGBD and where carbon-sequestration and conservation practices should acknowledge belowground-oriented carbon management. The recognition and valuation of biomass and carbon stocks beyond the AGBD is a must step forward that the scientific community must support in order to properly assess living components of the ecosystem such as root systems sustaining AGBD stocks and to value carbon-oriented ecosystem services related to soil-water dynamics and soil biodiversity. This study aims at enforcing a change of paradigm in forest carbon accounting, advocating for a better recognition and broader integration of living biomass in land carbon mapping.

1. Introduction

Aboveground biomass density (AGBD) is a flagship indicator for the monitoring of climate change effects over forests and carbon cycle

* Corresponding author.
E-mail address: apascual@umd.edu (A. Pascual).

http://dx.doi.org/10.1016/j.scitotenv.2023.165364
Received 28 April 2023; Received in revised form 4 July 2023; Accepted 4 July 2023
Available online 9 July 2023

dynamics (Pan et al., 2011; Saatchi et al., 2011; Schimel et al., 2015; Cook-Patton et al., 2020; Friedlingstein et al., 2022). Remote sensing is pivotal for monitoring AGBD stocks (Demol et al., 2022; Dubayah et al., 2022) and their accurate estimation is crucial to preserve forest biodiversity, to better invest in forest restoration or to strengthen the credibility of carbon sequestration projects (Maselli et al., 2009; Masciandaro et al., 2018). Forest biomass stocks are frequently expressed as AGBD only, and this excludes a large portion of the biomass budget. For an integrated assessment of forest biomass, we must start consistently informing on biomass in the belowground or in the forest floor. It is illogical from the optics of accounting to ignore measurable biomass components that elevates the portfolio of total forest biomass (Grassi et al., 2017; FAO, 2020; Gifford, 2020).

Global forest policies and monitoring systems should avoid the bias of looking only at AGB estimates to inform on total forest biomass stocks (Cook-Patton et al., 2020). Nowadays, it is mandatory for many countries to document both aboveground and belowground carbon stocks (FAO, 2020; Smith et al., 2020; López-Senespleda et al., 2021). Studies relating belowground biomass to measurable indicators of forest structure using remote sensing are scarce (Roudier et al., 2017; Lopatin et al., 2019; Ding et al., 2022). The increasing inclusion of belowground biomass data in National Forest Inventories (NFIs - Gschwantner et al., 2016; Guerra-Hernández et al., 2022) is a major support to maximize airborne laser scanning data (ALS) and estimate simultaneously above- and belowground biomass stocks, potentially improving maps derived from non-forest-specific sampling designs (Powers et al., 2011; Orgiazzi et al., 2018; Beland et al., 2019; Huang et al., 2019; FAO, 2020). For instance, the scale of 30 m - feasible and operational in contemporary AGBD maps supported with ALS data - exceeds the possibilities of coarser, global products for soil biomass based on empirical measurements (Powers et al., 2011; FAO, 2020).

Harmonized maps of different forest biomass stocks are necessary inputs to properly guide forest restoration and conservation (Magnússon et al., 2016; Luo et al., 2017; Anderson-Teixeira et al., 2018; Lopatin et al., 2019; Venter et al., 2021). The potential for biomass sequestration is frequently calculated using AGBD only assuming maximum biological stock potentially achievable just for the aboveground (Bastin et al., 2019; Pascual et al., 2021). In this study, we present an integrated evaluation of above- and belowground biomass stocks over almost 2 million ha of Mediterranean forests in Spain. We used airborne laser data to model AGBD using Spanish National Forest Inventory (SNFI) data of improved geolocation accuracy. Relations between above- and belowground biomass pools, and existing models to estimate litter biomass were used to map biomass stocks consistently at 25 m supported by ALS-based forest structural metrics. Selected forest types within the region were assessed to showcase different balances in biomass among the three modelled components. We calculated ratios at 25-m pixel scale to map areas where non-AGBD yield comparable stocks as the amount stored in the AGBD component. These ratios maps represent biomass dynamics and comprehensively inform on biomass and carbon storage across heterogenous landscapes.

2. Material and methods

2.1. Study area

The study area is Extremadura region (Central-West of Spain near Portugal) (Fig. 1), that covers 1.98 million ha of forest land (~47.6 % of the Extremadura region). These Mediterranean forests comprise old-growth forests of oaks in sparse conditions, ecosystems with dominance of Mediterranean pine trees or eucalypts, among others. Field measurements of tree structural attributes are systematically collected in the Spanish National Forest Inventory (SNFI-4, MAPA, 2018). The SNFI-4 measurements for Extremadura region date from 2017. In this study, we worked with all SNFI-4 dataset and a subset of plots of enhanced geolocation to better estimate AGBD. Measurements of tree diameter at breast height (dbh, cm) and tree height (m) were retrieved from the 768 plots, used for tree-level, species-specific aboveground biomass modelling (Ruiz-Peinado et al., 2011, 2012), later upscaled at 25-m plot-radius and expressed as aboveground density (AGBD, units in Mg ha^{-1}). The set of plots ranged over 15 forest types according to the Spanish National Forest Map (Table S1). Although the scope of the study is the estimation of total biomass stocks in the region, we made independent calculations for representative ecosystems (Table 1) represented with at least 50 samples in the SNFI-4 dataset.

2.2. Mapping AGBD using airborne laser data

Region-wide airborne laser scanning (ALS) using LiDAR technology – collected between October 2018 and July 2019 – was used to estimate AGBD using the SNFI-4 set of plots for calibration. Data collection parameters and properties of the LiDAR sensors can be found in Guerra-Hernández et al. (2022) and Pascual et al. (2020). The prediction of AGBD was done through ALS-based stratum-specific models (Table S2) using the enhanced-geolocation of a subset of SNFI-4 plots within the different strata of the Spanish Forest Map. At least one main tree species is represented in all strata. Shrub-dominated areas not defined as forests in the Spanish Forest Map were not used for the AGBD map – our AGBD estimates only inform on forest woody vegetation. Models using ALS-based statistics over SNFI-4 samples are present in Supplementary 2 for the five selected forest ecosystems. The strata-specific AGBD map at 25-m resolution is presented in Fig. 2.

2.3. Models for belowground biomass pools

2.3.1. Belowground biomass density (BGBD) estimates using SNFI-4 data

The 4th version of the SNFI includes plot-level estimates of root biomass (BGBD) using the allometric equations presented in Ruiz-Peinado et al., 2011; Ruiz-Peinado et al., 2012) for the main forest tree species in Spain. Some authors have used the approach of simultaneously calibrating AGBD and BGBD using remote sensing data (Ding et al., 2022; Venter et al., 2021). Others advocate for empirical relations to estimate the belowground (López-Senespleda et al., 2021). We followed the later as i) coppice systems or agro-forestry management for oak forests (dominant forest type in the region) have altered natural biomass accumulation dynamics across the region, and ii) we rely on the good performance of ALS-based estimation for the aboveground. Hence, we used a simple non-linear regression model (Eq. 1) to estimate root biomass (BGBD) as a function of AGBD.

$$BGBD = a\,AGBD^{b} \tag{1}$$

where *BGBD* is the root biomass estimated in SNFI-4 plots, *AGBD* is the aboveground biomass measured over the same plots (both expressed in Mg ha^{-1}) while *a* and *b* are the optimized model parameters in the regression fitting. We modelled five forest ecosystems independently and all SNFI-4 plot-data available (2142 samples) to provide a general region-specific model. We used all SNFI-4 plots available to increase the degrees of freedom during the fitting as co-registration between ALS and field positions does not affect the relation between biomass pools measured and SNFI-4 estimated. To measure the accuracy of the assumed relations, we used the relative root mean squared error (rRMSE) and adjusted R-squared (R^2).

2.3.2. Models for litter density (LD) estimation

The study from Montero et al. (2020) presents a collection of models to estimate LD in Spanish forests using structural predictors that can be derived from ALS point clouds. Forest cover (FC) is an example of a metric integrated in these LD models, derivable from ALS surveys and widely used as predictor of stocking variables such as basal area, volume and AGBD (Pascual et al., 2020; Guerra-Hernández et al., 2022). We used Montero et al. (2020)'s models (Eq. 2) using forest-type specific coefficients for the listed forest types in Table 2,

$$LBD = a\,e^{\left(b\,\sin^{-1}\left(\sqrt{\left(\frac{FC}{100}\right)}\right)\right.} \tag{2}$$

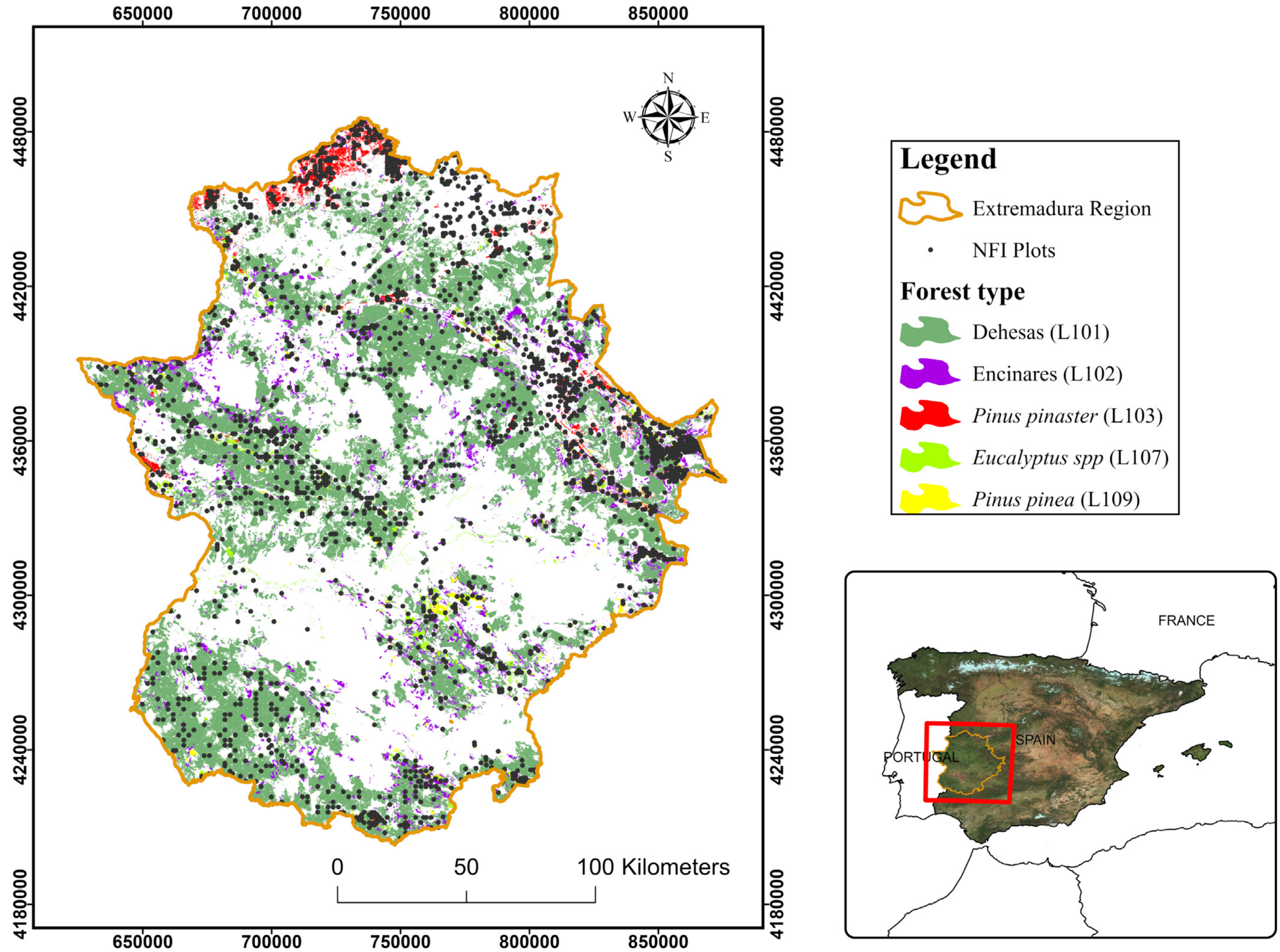

Fig. 1. Study area, SNFI-4 sampling plots and available aboveground carbon density map for region (25 m spatial resolution) built with ALS-based inference using SNFI-4 plots published by the authors in (Guerra-Hernández et al., 2022).

where *LD* is the amount of biomass litter expressed in Mg ha^{-1} measured in organic layers of the forest floor (fine wood debris, litter and humus) starting from the organic-upper layer (20 - 30 cm), *FC* is forest cover in the plot. The ALS-based calculation of FC is as follows: the ratio of ALS points ranging above 2 m and classified as first return (i.e., first hit of the laser pulse in the forest canopies) is expressed over the total number of ALS first returns ranging within the extent of each 25-m raster cell. We used it here to power Montero et al. (2020) model set and estimate LD at 25-m resolution for the entire region for which ALS data coverage is complete. Two general models for conifer and broadleaf tree species were available in Montero et al. (2020). We used those two models to estimate LD for the forest types not modelled independently (Table 2) but represented in the region of Extremadura.

Table 1
Summary table of the forest types evaluaed in this study in the training set of 768 plots. The table shows all strata and the five stratum for which the number of samples was more than 50.

Code	Forest type (FT) main species and description	Area (10^3 ha)
101	*Quercus* spp. – sparse old-growth oak forests (*Dehesas*)	1323.26
102	*Quercus ilex* subsp. *Ballota* (Desf.) Samp – less sparse conditions (*Encinares*)	196.05
103	*Pinus pinaster* spp. *hamiltonii* – Mediterranean resin pine forests	76.99
107	*Eucalypts* spp. –non-native eucalypts in different stages of development.	57.39
109	*Pinus pinea* L. – Mediterranean stone pine forests	30.66
All	The 15 stratum represented in the training data. See Annex I.	1973.65

2.4. Ratio maps to map the importance of biomass components

The three biomass components modelled were aggregated to compute the total biomass density (TBD). Mean and total values for the region were computed for all forest types and for the five selected showcases. The contribution of each biomass component was calculated at pixel-level (25-m resolution) and mapped for the entire region. The three ratio maps, one for each biomass component, represent insightful relative contributions of biomass.

3. Results

3.1. Estimation of root belowground biomass density (BGBD) using SNFI-4 data

The forest-type specific estimation of BGBD showed good predictive performance (Fig. 3, Suppl. 3). Combining all 2182 SNFI-4 observations for modelling turned out a low 0.36 value for R^2 and 20.6 Mg ha^{-1} as RMSE. However, forest-type specific results increased model performance above 0.8 R^2 for all forest type individually except for eucalypt stands. The later showed a weak linear relationship between predictor and response variable, aligned with general model using all SNFI data. Coppice

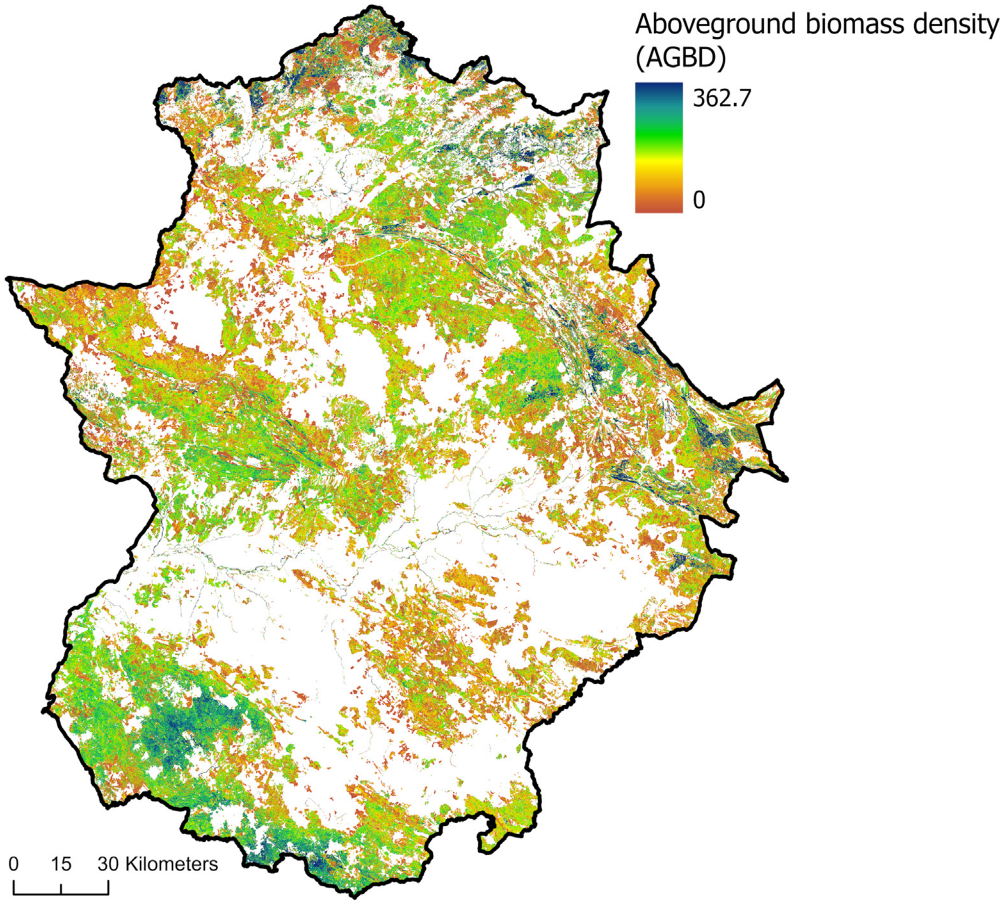

Fig. 2. Map of aboveground biomass density (AGBD, Mg ha^{-1}) available for Extremadura region created using airborne laser scanning data and National Forest Inventory data. The resolution of the AGBD product is 25 m. The models used to build the map is presented in Supplementary 2.

rotation systems and abandonment might have an influence for eucalypts as later discussed.

The presented models were applied over the 25-m AGBD product to predict BGBD over the study area using the boundaries as defined in the Forest Map of Spain. The average conditions for BGBD ranged between around 10 to 20 Mg ha^{-1}. The general model was applied for all 25-m AGBD pixels not ranging within the boundaries of the five selected forest types but within the region of Extremadura. Density functions comparing AGBD and BGBD predictions were computed to show the distribution of biomass (Fig. 4).

3.2. Prediction of litter biomass density (LD)

Model predictions for LD reached a maximum of 35 Mg ha^{-1} (Fig. 5). Differences between ecosystems were narrow: mean values ranged from 13.7 Mg ha^{-1} for *Pinus Pinea* forests (109) to 17.7 Mg ha^{-1} for the case of sparse *Quercus ilex* forests (forest type 101, Table 1) that is the most representative forest type in the area. The total litter biomass in the region was estimated in 41.8 million Mg - average value of 21.20 Mg ha^{-1}.

Table 2
Model coefficients used to predict litter biomass density (LD, Mg ha^{-1}) in the region. The general model for conifers and broadleaf tree species was used unless a foresty -type specific model was available in the set presented in Montero et al. (2020). Estimate values and the standard error reported by the authors are presented for both model parameters a and b included in Eq. 1.

Parameter	*a*		*b*	
Forest type	Estimate	Std. Error	Estimate	Std. Error
101 and 102	3.507	1.5833	1.166	0.4202
103	6.605	2.0093	0.757	0.2991
109	4.380	1.1832	0.978	0.2576
Conifer	3.808	0.4836	1.718	0.1115
Broadleaf	4.025	0.7025	1.073	0.1643

3.3. Total biomass density in the forest ecosystem

The aboveground component stocks 61.9 % of all biomass modelled, followed by belowground biomass (28.5 %) and litter (9.6 %). These percentages accrue 62.5 million Mg for aboveground biomass and 38.5 million Mg for the combination of belowground and litter biomass. Mean and total biomass estimates are presented in Table 3. The contribution of AGBD represents 52–68 % of all biomass in the forest types individually assessed. For instance, pine-dominated strata (forest types 103 and 109, Table 1) showed the largest contributions of AGBD: 68.3 % and 64.9 %, respectively. On the other hand, the lowest contribution from AGBD stocks was found for dense *Quercus ilex* stands (forest type 102) (52 %), showing the importance of belowground and litter biomass for this ecosystem. For the most represented forest type, open forests of *Quercus ilex* (forest type 101), the contribution of the aboveground biomass stock was estimated in 63 %.

3.4. Ratio-based maps for forest carbon-oriented management

Our interest was to quantify areas where AGBD mostly contributes to the biomass areas and areas where AGBD is below 50 % of the total TBD – showing the importance of belowground biomass and litter (Supplementary 4). We estimated that the contribution of AGBD exceeds 50 % of the total biomass in 41 % of all raster cells ranging within open forests of *Quercus ilex*. The value was higher for pine-dominated

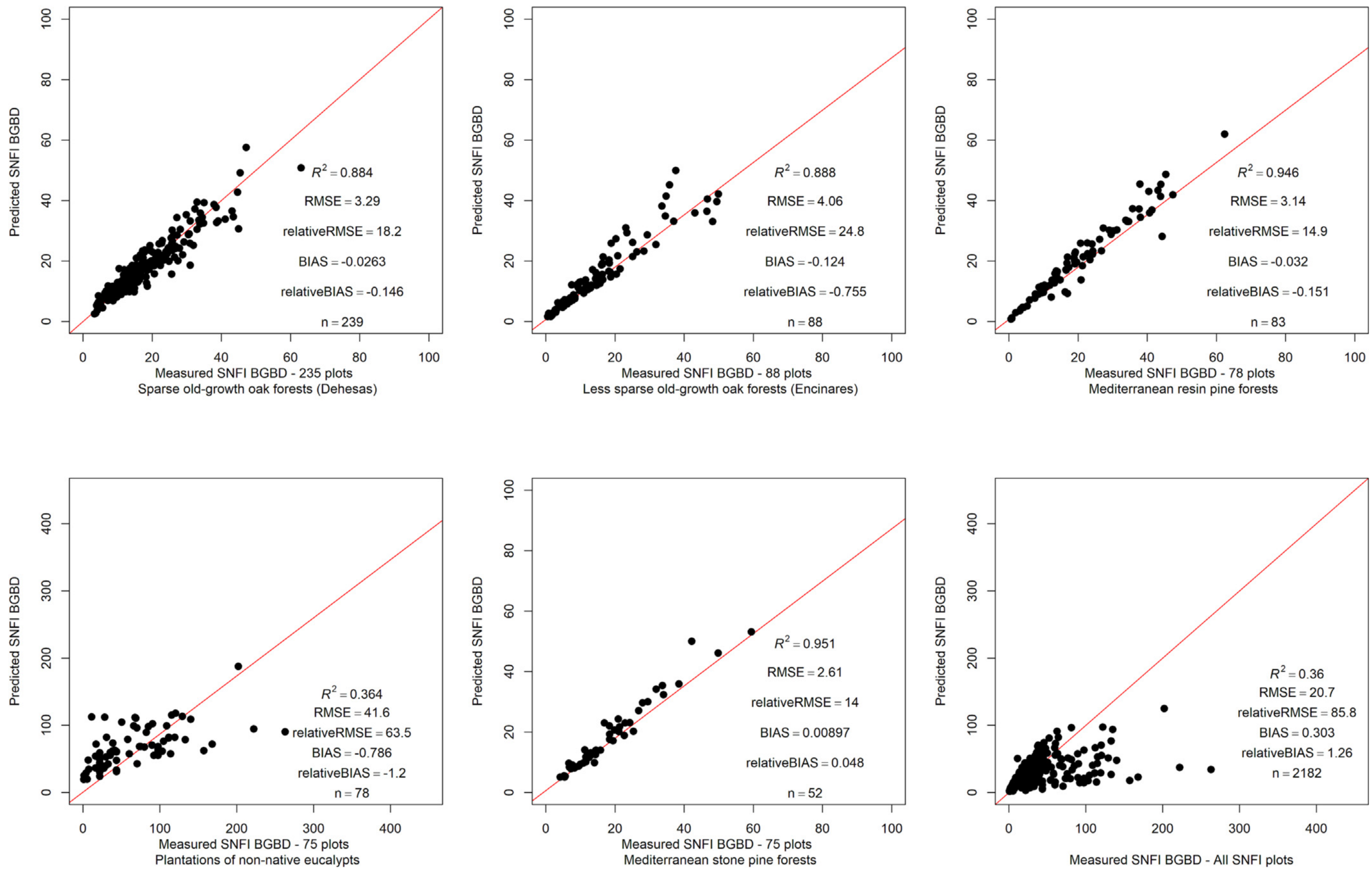

Fig. 3. Predicted versus measured belowground biomass (Mg ha^{-1}) stored in roots. Non-linear models are presented in the scatterplots together to fitting statistics. The relation was captured combining all NFI plots and separately for each of the five forest types selected.

forests: AGBD was the dominant contributor in *Pinus pinea* forests (62.8 %) and *Pinus pinaster* (54.9 %). These ratio maps help to identify patches and transitions between forest area showing different balances of biomass accumulation (Fig. 6).

4. Discussion

Our study evaluates and modelled aboveground, belowground and litter biomass using allometries built with reference data and ALS data. The ratio between above- and belowground biomass was species-specific and values were retrieved from official SNFI-4 reference plot data. The correlations (0.884–0.946) were strong as expected (Enquist and Niklas, 2002; Niklas, 2005; Cheng and Niklas, 2007; Hui et al., 2014). For instance, a study over a semi-arid woodland ecosystem (Handavu et al., 2019), which is structurally similar to sparse oaks, showed that the best model to predict BGBD was the one using the AGBD as predictor ($R^2 = 0.939$). We found a weak relation in eucalypts ($R^2 = 0.364$, Montero et al., 2020) and this can be explained by the abandonment in terms of silviculture or the switch to coppice systems that alters the natural accumulation of biomass (i.e., AGBD stocks is removed while roots keep growing). For the assessment of LD estimates, we looked at the data distribution of the training data used to calibrate the models from Montero et al. (2020): our mean estimates for forest types 102–109 ranged between 4.95 and 8.43 Mg ha^{-1}, similar to the values reported in the study. A good agreement was also observed for sparse oaks for which authors reported an average of 5.6 Mg ha^{-1}, close to our estimate (4.35 Mg ha^{-1}). Differences, although small, could be explained by discrepancies between field-based estimates of forest cover and the ALS-based estimates used here, or the limited sampling in Montero et al. (2020). We averaged model predictions over the whole extent of each forest type covering the complete gradient of FC, from 5 to 100 %, accurately captured with ALS data. Studies on the litter biomass in Mediterranean region, and in particular for the *Dehesas* ecosystem are scarce in the literature (e.g. Andivia et al., 2013).

Other studies have simultaneously estimated above- and belowground biomass pools. For instance, Luo et al. (2017) showed high agreement between biomass pools on an attempt to characterize total biomass supported by discrete airborne lidar data for the aboveground. The addition of climatic variables such as precipitation, temperature or time-series of water stress indicators are frequently explored as auxiliary data to improve the characterization of biomass dynamics as previous studies have tested using coarser scales (Saatchi et al., 2011; López-Senespleda et al., 2021; Ding et al., 2022). We preferred to use a simple, robust model between AGBD and BGBD – better model performance compared to i.e., Ding et al. (2022) and in line with in Luo et al. (2017) - without accounting for other auxiliary variables. We followed studies that have reported good performance using non-linear models to model relations between above- and belowground biomass (Soares and Tomé, 2012; Koala et al., 2017) while accounting for differences between forest types (Magnússon et al., 2016). The recent study from Devos et al. (2022) over Norway showed systematic differences between regions and eco-zones. The latter study reports mean root biomass values - expressed as C and not as biomass - of around 20 tons per ha, doubling our values.

The showcased area in Spain is representative of the Mediterranean basin and other forest biomes where belowground biomass and litter can substantially contribute to total ecosystem carbon. To better understand the different regimes in biomass accumulation for AGBD and BGBD in the region, it is important to acknowledge land-use and forest policy in the region. The use of oak forests as suppliers of firewood is important in the region and this has altered the accumulation of biomass in roots compared to the aboveground component, object of periodical removals to extract firewood (e.g. Andivia et al., 2013). Approximately 0.75 million ha of the *Dehesa* ecosystem (forest type 101) showed an AGBD ratio below 50 %,

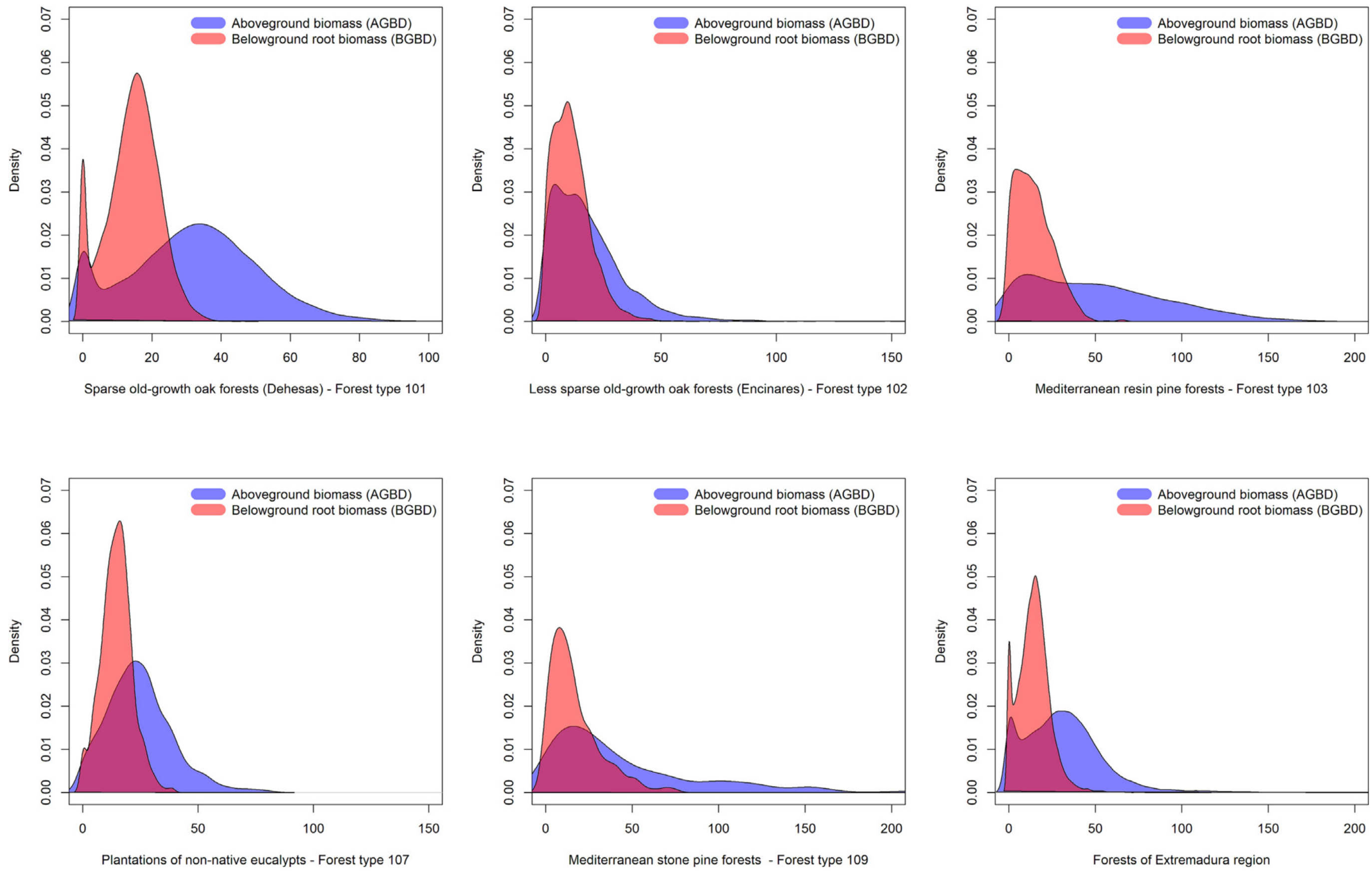

Fig. 4. Distribution of 25-m predictions of aboveground biomass density (AGBD) and belowground biomass density (BGBD) stored in roots across the study area. Both density functions are expressed in Mg ha^{-1}. Airborne laser scanning data and National Forest Inventory plots were used for calibration. Both density functions are presented for the five forests selected modelled separately and for all forest land in the region of Extremadura.

reflecting the importance of belowground biomass and litter on those areas, which should be take into consideration when designing land-use management policies. The study is based on ALS data and derived products such as canopy height models which strongly support the understanding of vegetation dynamics across the entire region. The presented biomass maps are driven by NFI data of enhanced geolocation for the calibrations which is key to model forest biomass with accuracy and reduce the impact of geolocation errors between laser statistics and reference biomass measurements. Our maps are tangible contributors to support environmental policy on climate change mitigation and also on wildfire management: the

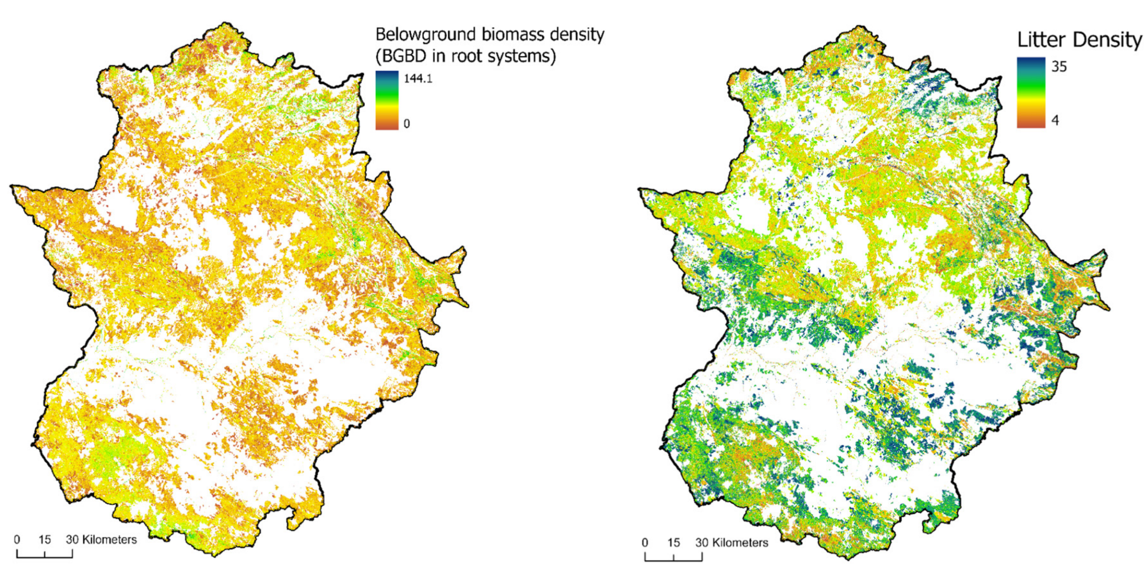

Fig. 5. Estimated belowground biomass density in root systems (BGBD, left) and estimated litter density (LD, right) expressed in Mg ha^{-1} at the spatial resolution of 25 m. For the second, models from Montero et al. (2020) were used for five selected forest types and a general model for conifers and broadleaf species for the rest of forests in Extremadura region.

Table 3
Mean and total values of carbon biomass density computed over the three components evaluated in the study; abroveground (AGBD), belowground (BGBD) and litter (LD). Results are presented for all forest area in Extremadura region (Spain) and specifically, for 5 forest types evalaued separately. The codes for Forest type definition are presented in Table 1.

Forest type	Aboveground biomass density (AGBD)		Belowground biomass density (BGBD)		Litter density (LD)	
	Mean Mg ha^{-1}	Totals 10^6 Mg	Mean Mg ha^{-1}	Totals 10^6 Mg	Mean Mg ha^{-1}	Totals 10^6 Mg
101	31.82	42.08	14.31	18.92	4.38	5.79
102	18.59	3.64	11.53	2.26	4.95	0.97
103	49.71	3.82	14.56	1.12	8.43	0.65
107	24.35	1.40	14.52	0.83	5.67	0.32
109	44.50	1.39	16.67	0.51	7.78	0.24
Ext (region)	31.63	62.52	14.59	28.79	4.85	9.7

mapped biomass stocks are useful i.e., to sequence fuel treatments on areas where aboveground stocks are high, and also to value C losses from wildfires on three biomass components.

5. Conclusions

We now have the science to map different biomass components. Airborne lidar is a solid support for the estimation of aboveground carbon pools but also to belowground components as long as allometries are built considering measurable metrics from the aboveground. Here we showcased one example in Spain to model three biomass components at the same scale and making use of publicly available data. The very-much AGBD-focused policies to promote restoration and responsible land stewardship must start acknowledging belowground biomass stocks for a fair recognition of the multiple biomass components in a forest. We hope belowground biomass components become more and more included into global biomass reports for a comprehensive and inclusive approach to model forest biomass stocks.

Author contributions statement

Adrián Pascual: Conceptualization, Investigation, Formal analysis, Model formulation, Visualization and Writing – original draft, review and editing.

Juan Guerra-Hernández: Formal analysis and Writing.

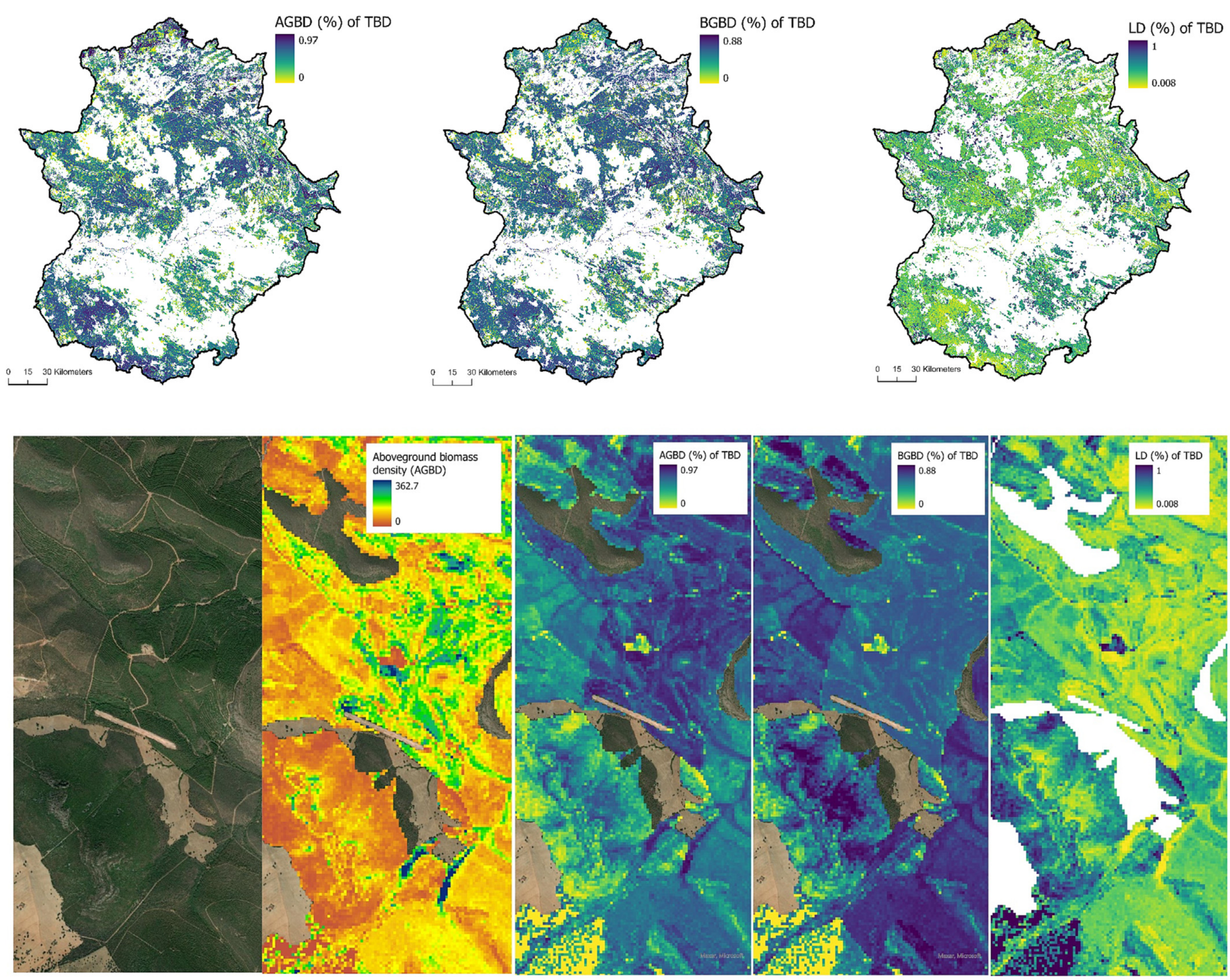

Fig. 6. Contribution of aboveground biomass density (AGBD), belowground biomass density in roots (BGBD) and litter density (LD) to the sum computed at 25-m pixel level. Maps presented for the region of Extremadura in Spain and showcased for a 12-km^2 transect to illustrate changes in the different contribution to the total aggregated biomass.

Funding

This research was supported by the grant funded by the Foundation for Science and Technology (FCT), Portugal to Dr. Guerra- Hernández (#CEECIND/02576/2022). This research was supported by the project "Extensión del cuarto inventario forestal nacional mediante técnicas LiDAR para la gestión sostenible de los montes de Extremadura" from the Extremadura Forest Service (FEADER no. 1952SE1FR435). Sérgio Godinho was supported by the FUEL-SAT project "Integration of multi-source satellite data for wildland fuel mapping: the role of remote sensing for an effective wildfire fuel management" from Foundation for Science and Technology (FCT) (PCIF/GRF/0116/ 2019).

Data availability

Data will be made available on request.

Declaration of competing interest

The authors declare that they have no known competing financial interests or personal relationships that could have appeared to influence the work reported in this paper.

Acknowledgements

We acknowledge Spanish National Forest Inventory (SNFI) from MAPA for making the ground data of the 4th round (SNFI-4) available to us to conduct the study. We acknowledge the importance of the publicly available ALS data from the PNOA project in Spain for our study. The authors also thank to Forest Research Centre, a research unit funded by Fundação para a Ciência e Tecnologia I.P. (FCT), Portugal (UIDB/00239/2023).

Appendix A. Supplementary data

Supplementary data to this article can be found online at https://doi.org/10.1016/j.scitotenv.2023.165364.

References

Anderson-Teixeira, K.J., Wang, M.M.H., McGarvey, J.C., Herrmann, V., Tepley, A.J., Bond-Lamberty, B., LeBauer, D.S., 2018. ForC: a global database of forest carbon stocks and fluxes. Ecology 99 (6), 1253–1512. https://doi.org/10.1002/ecy.2229.
Andivia, E., Vásquez-Piqué, J., Fernandéz, M., Alejano, R., 2013. Litter production in holm oak trees subjected to different pruning intensities in Mediterranean dehesas. Agrofor. Syst. 87, 657–666. https://doi.org/10.1007/s10457-012-9586-5.
Bastin, J.-F., Finegold, Y., Garcia, C., Mollicone, D., Rezende, M., Routh, D., Zohner, C.M., Crowther, T.W., 2019. The global tree restoration potential. Science 365 (6448), 76–79. https://doi.org/10.1126/science.aax0848.
Beland, M., Parker, G., Sparrow, B., Harding, D., Chasmer, L., Phinn, S., Antonarakis, A., Strahler, A., 2019. On promoting the use of lidar systems in forest ecosystem research. For. Ecol. Manag. 450, 117484. https://doi.org/10.1016/j.foreco.2019.117484.
Cheng, D., Niklas, K., 2007. Above- and below-ground biomass relationships across 1534 forested communities. Annals Botany 99, 95–102. https://doi.org/10.1093/aob/mcl206.
Cook-Patton, S.C., Leavitt, S.M., Gibbs, D., Harris, N.L., Lister, K., Anderson-Teixeira, K.J., Briggs, R.D., Chazdon, R.L., Crowther, T.W., Ellis, P.W., Griscom, H.P., Herrmann, V., Holl, K.D., Houghton, R.A., Larrosa, C., Lomax, G., Lucas, R., Madsen, P., Malhi, Y., Griscom, B.W., 2020. Mapping carbon accumulation potential from global natural forest regrowth. Nature 585 (7826), 545–550. https://doi.org/10.1038/s41586-020-2686-x.
Demol, M., Verbeeck, H., Gielen, B., Armston, J., Burt, A., Disney, M., Duncanson, L., Hackenberg, J., Kükenbrink, D., Lau, A., Ploton, P., Sewdien, A., Stovall, A., Takoudjou, S.M., Volkova, L., Weston, C., Wortel, V., Calders, K., 2022. Estimating forest above-ground biomass with terrestrial laser scanning: current status and future directions. Methods Ecol. Evol. 13 (8), 1628–1639. https://doi.org/10.1111/2041-210X.13906.
Devos, C.C., Ohlson, M., Næsset, E., Bollandsås, O.M., 2022. Soil carbon stocks in forest-tundra ecotones along a 500 km latitudinal gradient in northern Norway. Sci. Rep. 12 (1), 13358. https://doi.org/10.1038/s41598-022-17409-3.
Ding, L., Li, Z., Shen, B., Wang, X., Xu, D., Yan, R., Yan, Y., Xin, X., Xiao, J., Li, M., Wang, P., 2022. Spatial patterns and driving factors of aboveground and belowground biomass over the eastern Eurasian steppe. Sci. Total Environ. 803, 149700. https://doi.org/10.1016/j.scitotenv.2021.149700.
Dubayah, R., Armston, J., Healey, S.P., Bruening, J.M., Patterson, P.L., 2022. GEDI launches a new era of biomass inference from space GEDI launches a new era of biomass inference from space. Environ. Res. Lett. Lett. 17, 095001. https://doi.org/10.31223/X52W68.
Enquist, B.J., Niklas, K.J., 2002. Global allocation rules for patterns of biomass partitioning across seed plants. Science 295, 1517–1520. https://doi.org/10.1126/science.1066360.
FAO, 2020. In: Peralta, G., Di Paolo, L., Omuto, C., Viatkin, K., Luotto, I., Yigini, Y. (Eds.), GSOCseq Global Soil Organic Carbon Sequestration Potential Map Technical Manual, 1st edition Rome. Available at https://fao-gsp.github.io/GSOCseq/.
Friedlingstein, P., Jones, M.W., O'Sullivan, M., Andrew, R.M., Bakker, D.C.E., Hauck, J., Le Quéré, C., Peters, G.P., Peters, W., Pongratz, J., Sitch, S., Canadell, J.G., Ciais, P., Jackson, R.B., Alin, S.R., Anthoni, P., Bates, N.R., Becker, M., Bellouin, N., Zeng, J., 2022. Global carbon budget 2021. Earth Syst. Sci. Data 14 (4), 1917–2005. https://doi.org/10.5194/essd-14-1917-2022.
Gifford, L., 2020. You can't value what you can't measure: a critical look at forest carbon accounting. Clim. Chang. 161 (2), 291–306. https://doi.org/10.1007/s10584-020-02653-1.
Grassi, G., House, J., Dentener, F., Federici, S., den Elzen, M., Penman, J., 2017. The key role of forests in meeting climate targets requires science for credible mitigation. Nat. Clim. Chang. 7 (3), 220–226. https://doi.org/10.1038/nclimate3227.
Gschwantner, T., Lanz, A., Vidal, C., Bosela, M., Di Cosmo, L., Fridman, J., Gasparini, P., Kuliešis, A., Tomter, S., Schadauer, K., 2016. Comparison of methods used in European National Forest Inventories for the estimation of volume increment: towards harmonisation. Ann. For. Sci. 73 (4), 807–821. https://doi.org/10.1007/s13595-016-0554-5.
Guerra-Hernández, J., Botequim, B., Bujan, S., Jurado-Varela, A., Molina-Valero, J.A., Martínez-Calvo, A., Pérez-Cruzado, C., 2022. Interpreting the uncertainty of model-based and design-based estimation in downscaling estimates from NFI data: a case-study in Extremadura (Spain). GIScience & Remote Sensing 59 (1), 686–704. https://doi.org/10.1080/15481603.2022.2051383.
Handavu, F., Syampungani, S., Sileshi, G.W., Chirwa, P.W.C., 2019. Aboveground and below-ground tree biomass and carbon stocks in the miombo woodlands of the Copperbelt in Zambia. Carbon Manage. 12 (3), 307–321. https://doi.org/10.1080/17583004.2021.1926330.
Huang, H., Liu, C., Wang, X., Zhou, X., Gong, P., 2019. Integration of multi-resource remotely sensed data and allometric models for forest aboveground biomass estimation in China. Remote Sens. Environ. 221, 225–234. https://doi.org/10.1016/j.rse.2018.11.017.
Hui, D., Wang, J., Shen, W., Le, X., Ganter, P., Ren, H., 2014. Near isometric biomass partitioning in forest ecosystems of China. PLoS One 9, e86550. https://doi.org/10.1371/journal.pone.0086550.
Koala, J., Sawadogo, L., Savadogo, P., Aynekulu, E., Heiskanen, J., Saïd, M., 2017. Allometric equations for below-ground biomass of four key woody species in west African savanna-woodlands. Silva Fennica 51 (3). https://doi.org/10.14214/sf.1631.
Lopatin, J., Kattenborn, T., Galleguillos, M., Perez-Quezada, J.F., Schmidtlein, S., 2019. Using aboveground vegetation attributes as proxies for mapping peatland belowground carbon stocks. Remote Sens. Environ. 231, 111217. https://doi.org/10.1016/j.rse.2019.111217.
López-Senespleda, E., Calama, R., Ruiz-Peinado, R., 2021. Estimating forest floor carbon stocks in woodland formations in Spain. Sci. Total Environ. 788, 147734. https://doi.org/10.1016/j.scitotenv.2021.147734.
Luo, S., Wang, C., Xi, X., Pan, F., Peng, D., Zou, J., Nie, S., Qin, H., 2017. Fusion of airborne LiDAR data and hyperspectral imagery for aboveground and belowground forest biomass estimation. Ecol. Indic. 73, 378–387. https://doi.org/10.1016/j.ecolind.2016.10.001.
Magnússon, R.Í., Tietema, A., Cornelissen, J.H.C., Hefting, M.M., Kalbitz, K., 2016. Tamm review: sequestration of carbon from coarse woody debris in forest soils. For. Ecol. Manag. 377, 1–15. https://doi.org/10.1016/j.foreco.2016.06.033.
MAPA, 2018. Mapa Forestal de España. Escala 1:25.000. Ministerio de Agricultura,Pesca y Alimentación. Dirección General de Desarrollo Rural, Innovación y Política Forestal. Link.
Masciandaro, G., Macci, C., Peruzzi, E., Doni, S., 2018. Soil carbon in the world: Ecosystem services linked to soil carbon in Forest and agricultural soils. The Future of Soil Carbon. Elsevier, pp. 1–38. https://doi.org/10.1016/B978-0-12-811687-6.00001-8.
Maselli, F., Chiesi, M., Moriondo, M., Fibbi, L., Bindi, M., Running, S.W., 2009. Modelling the forest carbon budget of a Mediterranean region through the integration of ground and satellite data. Ecol. Model. 220 (3), 330–342. https://doi.org/10.1016/j.ecolmodel.2008.10.002.
Montero, G., Lopez-Leiva, C., Ruiz-Peinado, R., Lopez-Senespleda, E., Onrubia, R., Pasalodos-Tato, M. (2020). Producción de biomasa y fijación de carbono por los matorrales españoles y por el horizontes orgánico superficial de los suelos forestales. {In Spanish}. Ministerio de Agricultura, Pesca y Alimentación. Available: https://www.mapa.gob.es/es/desarrollo-rural/publicaciones/.
Niklas, K.J., 2005. Modelling below- and above-ground biomass for non-woody and woody plants. Ann. Bot. 95, 315–321. https://doi.org/10.1093/aob/mci028.
Orgiazzi, A., Ballabio, C., Panagos, P., Jones, A., Fernández-Ugalde, O., 2018. LUCAS soil, the largest expandable soil dataset for Europe: a review. Eur. J. Soil Sci. 69 (1), 140–153. https://doi.org/10.1111/ejss.12499.
Pan, Y., Birdsey, R.A., Fang, J., Houghton, R., Kauppi, P.E., Kurz, W.A., Phillips, O.L., Shvidenko, A., Lewis, S.L., Canadell, J.G., Ciais, P., Jackson, R.B., Pacala, S.W., McGuire, A.D., Piao, S., Rautiainen, A., Sitch, S., Hayes, D., 2011. A large and persistent carbon sink in the World's forests. Science 333 (6045), 988–993. https://doi.org/10.1126/science.1201609.
Pascual, A., Guerra-Hernández, J., Cosenza, D.N., Sandoval, V., 2020. The role of improved ground positioning and Forest structural complexity when performing Forest inventory using airborne laser scanning. Remote Sens. 12, 413. https://doi.org/10.3390/rs12030413.
Pascual, A., Giardina, C.P., Selmants, P.C., Laramee, L.J., Asner, G.P., 2021. A new remote sensing-based carbon sequestration potential index (CSPI): a tool to support land carbon management. For. Ecol. Manag. 494, 119343. https://doi.org/10.1016/j.foreco.2021.119343.
Powers, J.S., Corre, M.D., Twine, T.E., Veldkamp, E., 2011. Geographic bias of field observations of soil carbon stocks with tropical land-use changes precludes spatial extrapolation. Proc. Natl. Acad. Sci. 108 (15), 6318–6322. https://doi.org/10.1073/pnas.1016774108.

Roudier, P., Malone, B.P., Hedley, C.B., Minasny, B., McBratney, A.B., 2017. Comparison of regression methods for spatial downscaling of soil organic carbon stocks maps. Comput. Electron. Agric. 142, 91–100. https://doi.org/10.1016/j.compag.2017.08.021.

Ruiz-Peinado, R., del Rio, M., Montero, G., 2011. New models for estimating the carbon sink capacity of Spanish softwood species. Forest Systems 20, 176–188. https://doi.org/10.5424/fs/2011201-11643.

Ruiz-Peinado, R., González, G.M., Del Rio, M., 2012. Biomass models to estimate carbon stocks for hardwood tree species. Forest Systems 21, 42–52. https://doi.org/10.5424/fs/2112211-02193.

Saatchi, S.S., Harris, N.L., Brown, S., Lefsky, M., Mitchard, E.T.A., Salas, W., Zutta, B.R., Buermann, W., Lewis, S.L., Hagen, S., Petrova, S., White, L., Silman, M., Morel, A., 2011. Benchmark map of forest carbon stocks in tropical regions across three continents. Proc. Natl. Acad. Sci. 108 (24), 9899–9904. https://doi.org/10.1073/pnas.1019576108.

Schimel, D., Pavlick, R., Fisher, J.B., Asner, G.P., Saatchi, S., Townsend, P., Miller, C., Frankenberg, C., Hibbard, K., Cox, P., 2015. Observing terrestrial ecosystems and the carbon cycle from space. Glob. Chang. Biol. 21 (5), 1762–1776. https://doi.org/10.1111/gcb.12822.

Smith, P., Soussana, J., Angers, D., Schipper, L., Chenu, C., Rasse, D.P., Batjes, N.H., Egmond, F., McNeill, S., Kuhnert, M., Arias-Navarro, C., Olesen, J.E., Chirinda, N., Fornara, D., Wollenberg, E., Álvaro-Fuentes, J., Sanz-Cobena, A., Klumpp, K., 2020. How to measure, report and verify soil carbon change to realize the potential of soil carbon sequestration for atmospheric greenhouse gas removal. Glob. Chang. Biol. 26 (1), 219–241. https://doi.org/10.1111/gcb.14815.

Soares, P., Tomé, M., 2012. Biomass expansion factors for Eucalyptus globulus stands in Portugal. Forest Systems 21 (1), 141. https://doi.org/10.5424/fs/2112211-12086.

Venter, Z.S., Hawkins, H.-J., Cramer, M.D., Mills, A.J., 2021. Mapping soil organic carbon stocks and trends with satellite-driven high-resolution maps over South Africa. Sci. Total Environ. 771, 145384. https://doi.org/10.1016/j.scitotenv.2021.145384.